The Innovation, Volume *2*

Supplemental Information

Geochemical provenancing and direct dating of the Harbin archaic human cranium

Qingfeng Shao, Junyi Ge, Qiang Ji, Jinhua Li, Wensheng Wu, Yannan Ji, Tao Zhan, Chi Zhang, Qiang Li, Rainer Grün, Chris Stringer, and Xijun Ni

SUPPLEMENTAL INFORMATION

Title:

Geochemical provenancing and direct dating of the Harbin archaic human cranium

Authors list:

Qingfeng Shao[1,12], Junyi Ge[2, 3,12], Qiang Ji[4*], Jinhua Li[5], Wensheng Wu[4], Yannan Ji[6], Tao Zhan[7], Chi Zhang[2, 3], Qiang Li[2, 3], Rainer Grün[8,9*], Chris Stringer[10*], Xijun Ni[2, 3, 4, 11*]

Affiliations:

1. Key Laboratory of Virtual Geographic Environment, Ministry of Education, Nanjing Normal University, Nanjing, 210023, China
2. CAS Center for Excellence in Life and Paleoenvironment, Chinese Academy of Science, Beijing, 100044, China
3. University of Chinese Academy of Sciences, Beijing, 100049, China
4. Hebei GEO University, Shijiazhuang, Hebei Province, 050031, China
5. Key Laboratory of Earth and Planetary Physics, Innovation Academy for Earth Science, Chinese Academy of Sciences, Beijing 100029, China
6. China Geo-Environmental Monitoring Institute, Beijing, 100081, China
7. The Second Hydrogeology and Engineering Geology Prospecting Institute of Heilongjiang Province, Harbin 150030, China
8. Australian Research Centre for Human Evolution, Griffith University, Nathan, Queensland, Australia
9. Research School of Earth Sciences, The Australian National University, Canberra, ACT, Australia
10. Centre for Human Evolution Research, Department of Earth Sciences, Natural History Museum, London, UK
11. CAS Center for Excellence in Tibetan Plateau Earth Sciences, Chinese Academy of Science, Beijing, 100104, China
12. Co-first authors

Correspondence:

* nixijun@hgu.edu.cn (X.N.); jiqiang@hgu.edu.cn (Q.J.); rainer.grun@griffith.edu.au (R.G.); c.stringer@nhm.ac.uk (C.S.)

Regional Stratigraphy

The Quaternary lithostratigraphy in the Harbin region include 5 units from the top to the bottom[1-3]: Tantu Formation, Guxiangtun Formation, Harbin Formation, Upper Huangshan Formation and Lower Huangshan Formation (Fig. 1). The uppermost Tantu Formation spreads on the floodplain of Songhua River mainly west to the Harbin city. The formation consists of a series of Holocene dark brown, grayish brown and grayish black alluvial- fluvial clay and sandy clay. The Guxiangtun Formation consists of yellowish brown, grayish brown, and grayish black silty clay, loess and sandstone of fluvial-lacustrine origin. The formation is widely distributed on the lower terraces or higher floodplains of the Songhua River. The upper part of the Guxiangtun Formation includes mainly dark brown or grayish black clay, and yellowish brown loess with bends of palaeosoil. The lower part of the Guxiangtun Formation includes reworked loess, dark brown and grayish black sandy clay, silt and clay. There are a large amount of charcoal grains in the lower part of the formation. The age of this formation is between ~12 ka and ~79 ka[2]. The Harbin Formation consists of mainly yellowish-brown and yellow aeolian loess with bends of paleosoils. The formation is partially exposed on the lower terrace of the Songhua River and parts of the floodplain in the Harbin region. The formation was recently dated between ~138 ka and ~79 ka[2]. The Upper Huangshan Formation is characterized by greenish-gray, grayish-brown, and dark gray muddy siltstone or silty mudstone with a few lenticular fine sandstone layers of fluvial-lacustrine origins. The age of the Upper Huangshan Formation is between ~580 ka and ~138 ka[2]. This formation is mainly distributed on the higher terrace or on the piedmonts in the east and northeast areas of Songhua River floodplain. The Upper Huangshan Formation overlays the Lower Huangshan Formation. The upper part of the Lower Huangshan Formation mainly consists of brownish-gray to dark gray lacustrine sandy mudstone. The lower part of the Lower Huangshan Formation is a set of grayish-brown or yellowish-brown fluvial sandstone. The Lower Huangshan Formation is scarcely exposed at a few thick sediment sections[2, 4]. The uppermost Lower Huangshan Formation is currently dated as ~580 ka[2]. The bottom of the Lower Huangshan Formation is not exposed. It is believed that the whole formation belongs to the late Early Pleistocene and early Middle Pleistocene[2, 4].

The five formations are all fossiliferous. The whole area is indeed one of the most fossiliferous areas in China. Mammalian fossils from the Guxiangtun Formation and the Upper Huangshan Formation are extremely common. Thousands of mammalian fossils and many human fossils were collected from the underwater sand mine sites in the Songhua River near the Harbin City. Because the mining activities are well monitored and controlled, it is clear now that these fossils are mainly collected from the sediments of the Guxiangtun Formation and the upper part of the Upper Huangshan Formation of these underwater sand mine sites. More than 70 species have been reported from the area[5-11].

X-Ray fluorescence (XRF) analyses.

XRF analyses were performed on the M4 TORADO PLUS Micro-SRF analyzer at the Institute of Geology and Geophysics, Chinese Academy of Sciences, following the procedures of Li et al. [12]. In order to avoid system error caused by the measurement setting and the unevenness

of the test region, one area of about ~1-2 cm^2 for each sample was randomly selected for collecting the XRF signals according to the same measuring parameters (i.e., the high voltage is 50 kV, and the pixel size is 40 μm). For semi-quantitative comparisons, each XRF spectrum was normalized with the signal of Rh-Lα peak, which is generated by a Rh X-ray source.

The samples used for comparison include a black bear mandible, a bison carpal, a bison maxilla, a red deer carpal, a mammoth tooth, and a marmot mandible. Two control samples were also included: a rhinoceros mandible recovered from Jiangsu Province and a rhinoceros maxilla recovered from Guangxi Province. The two specimens were recovered from similar Pleistocene fluvial underwater sediments as that of the Harbin cranium, but the sediments belong to different drainage areas and have different depositional sources. All the mammalian fossils are housed in the Institute of Vertebrate Paleontology and Paleoanthropology, Beijing, China.

HR-ICP-MS Rare earth element (REE) analyses.

Small bone pieces (100 mg) from the nasal cavity of the Harbin cranium were carefully collected for REE and Sr isotopic analyses. For comparison, fossil fragments from seven mammals and two human individuals recovered from the Harbin area in the Songhua River were also analyzed. The age of these fossils ranges from the Middle Pleistocene to the Early Holocene (S-Fig.1,2; S-Table 1). All the fossils are deposited in the Institute of Vertebrate Paleontology and Paleoanthropology.

REE analyses were performed at the State Key Laboratory for Mineral Deposits Research, Nanjing University. The samples were processed using the method of Ref. [13]. In the laboratory, after removal of the surface contaminations using the dental drill and ultrasonically washing in the ultrapure (18.2 MΩ/cm) water, bone samples were dried and ground into powder with a mortar and pestle. The resulting powder was soaked in a pH 5 acetic acid-ammonium acetate buffer for 1 h to remove the authigenic carbonates and centrifugated and dried at 60°C overnight. About 20 mg of each sample was weighed and dissolved in 2 mL 20% HNO_3 for REE measurements. The prepared sample solutions were diluted with 2% HNO_3 by a factor of 10 before analyses. The REE concentrations were determined using a HR-ICP-MS (high resolution inductively coupled plasma mass spectrometer). The rhodium solution (10 ppb) was dropped into the sample solutions for instrument drift correction. Analytical precision was <5% for each element.

MC-ICPMS strontium (Sr) isotopic analyses

Sr isotopic analyses were performed on the fossil samples from the Harbin cranium (n=1), the Middle Pleistocene-Early Holocene mammalian fossils (S-Fig.1; S-Table 2; n=7) and human fossils (S-Fig. 2; S-Table 2; n=2) recovered from the Harbin area in the Songhua River. The sediment samples adhering to the nasal cavity of the Harbin cranium (n=1) and from a core (n=40) drilled near the Dongjiang Bridge (Fig. 1) were also analyzed. The Sr isotopic analyses were carried out at the Nanjing Normal University with a MC-ICPMS (multicollector inductively coupled plasma mass spectrometer, Thermo Fisher Neptune). Sample preparation and measure methods followed those of Ref. [14]. Samples were crushed using a mortar and pestle and cleaned

of carbonate using pH 5 acetic acid-ammonium acetate buffer. Approximately 1 mg bone powder was weighed in a 30 mL Teflon beaker and dissolved in trace-metal grade HNO_3. For sediment samples, about ~50 mg of each powdered sediment was weighed and digested using high-purity HNO_3 (1 mL) and HF (1.5 mL) for 72 h in a tightly closed Teflon vessel in an oven at 190°C. The sample solution was evaporated to dryness on a hotplate at 160°C. Dry sediment samples were repeatedly reacted with 1 mL concentrate HNO_3 to remove residual HF. All sample solutions were then evaporated to dryness, and the residues were dissolved with 0.5 mL of 3N HNO_3 at 96°C to change the medium for sample loading. The column (capacity of 1 mL) packed with 0.1 mL Sr-spec resin was used to separate Sr from other ions. The column was rinsed with 1 mL of 6N HCl and Milli-Q water to wash the residual Sr and other ions. After conditioning with 3N HNO_3, the sample solution was loaded onto the column. Sr was then eluted with 0.05 N HNO_3 and collected to evaporate to dryness. The residue was dissolved with 2% HNO_3 prior to measurements.

The samples were introduced through a nominally 50 μL min-1 capillary tube and aspirated into a Cetac Aridus II desolvating chamber running at 110°C. The Sr isotope measurement were conducted on a MC-ICPMS (Thermo Fisher Neptune). The measured $^{87}Sr/^{86}Sr$ ratio was corrected for mass fractionation by normalization to a constant $^{86}Sr/^{88}Sr$ ratio of 0.1194 using an exponential law. The isobaric interference of ^{87}Rb on ^{87}Sr was corrected using a natural $^{87}Rb/^{85}Rb$ ratio of 0.3857. Replicate measurements of the NIST SRM 987 standard yielded mean value of $^{87}Sr/^{86}Sr$ =0.710263±0.000014 (2σ, n=11) during the analytical period (S-Table 2) which is in good agreement with the data in the literature [15, 16].

The Sr isotope ratios of the Harbin cranium and mammalian/human fossils in comparions all fall into the variation range of the regional bioavailable Sr isotope ratio values in the Harbin areas (S-Fig. 3). Compared with other areas of China, the Harbin and nearby areas have the lowest bioavailable Sr isotope ratios.

MC-ICPMS Uranium-series analyses

The U-series dating samples (n = 10) were hand-drilled on the Harbin cranium with 0.3 mm carbide-tipped drill bits. To minimize destruction on the cranium, the powder sample size was kept between 0.1-0.5 mg. The locations selected for sampling all have relatively fresh bone surfaces without visible porosity. Before sampling, the bone surface was abraded to remove any superficial contamination. The powdered sample was first collected on a weighing paper, and then transferred into a clean centrifuge tube (2 ml in volume). To determine the weight of the powdered sample, the centrifuge tube was weighed before and after the sample collection with an analytical balance.

The U-series dating analyses were carried out at the Nanjing Normal University (NNU). The powdered samples were dissolved in 3N HNO_3 in a centrifuge tube, and then transferred into a Teflon beaker containing a known quantity of a ^{229}Th-^{233}U-^{236}U triple spike. One drop of $HClO_4$ was added to the sample solution to decompose organic material. The sample-spike mixture was heated overnight on a hot plate at 120°C. After the equilibration of the sample-spike mixture, U and Th were separated from each other and from other cations by passing the sample solution

through a U-TEVA resin column following the procedure of Douville et al. [17]. Firstly, the sample matrix elements were eliminated through rinsing with 3N HNO_3. Subsequently, Th was eluted using 3N HCl, and finally U was eluted using 0.5N HCl. One drop of $HClO_4$ was added to the U or Th fractions to remove any organic material derived from the U-TEVA resins. The U and Th solutions were evaporated to dryness and then dissolved in a mixture of 0.5 N HNO_3 and 0.01 N HF for U and Th isotopic analyses.

The U and Th isotopic measurements were performed on a MC-ICPMS (Thermo Fisher Neptune). It is equipped with nine Faraday cups and a secondary electron multiplier (SEM). A retarding potential quadrupole (RPQ) energy filter was positioned in front of the SEM. An Aridus-II desolvator system (Cetac) coupled with an ESI-50 nebulizer and an AutoSampler (ASX-520) were used for sample introduction. The U-Th data acquisition strategies applied here were similar to those described by Shao et al. [18]. The U isotopic data were acquired in two static sequences. The first sequence measured ^{233}U, ^{235}U, ^{236}U and ^{238}U in cups and simultaneously ^{234}U on the SEM (with RPQ-on). The second sequence shifted all masses by 1 amu to the lower mass, so that ^{233}U was measured by the SEM and the other isotopes by the cups. Thorium measurements were carried out immediately after the uranium measurements for the same sample. ^{229}Th and ^{230}Th were measured alternately on the SEM (with RPQ-on) and ^{232}Th in a cup. The U isotopes of the HU-1 standard solution were measured after every 2 samples to monitor instrumental stability.

The amplifier gains, dark noise, hydride interferences and machine abundance sensitivity were evaluated every day prior to the sample measurements. The base lines were automatically calibrated before each U isotopic measurement. Instrument memory was assessed with the SEM by introducing a blank solution before measurements of either U or Th were conducted. The relative yields of the SEM/Faraday cups were determined during U isotopic measuring by alternating the ^{233}U beam (~5 mV) on the SEM and in the Faraday cup. Instrumental mass fractionation was corrected by using an exponential function comparing the measured $^{238}U/^{235}U$ with the natural value of 137.82 for unknown samples [19]. Procedural blank was corrected by using the long-term observed values of ~0.8 fg ^{234}U, ~10 pg ^{238}U, ~0.1 fg ^{230}Th and ~2.0 pg ^{232}Th, respectively. The U-series ages (expressed here as years before 2000 A.D., b2k) were calculated by Monte-Carlo simulations[31], using half-lives of 75,584 yr for ^{230}Th[20] and 245,620 yr for ^{234}U[20], 1.4×10^{10} yr for ^{232}Th[21], and 4.47×10^{9} yr for ^{238}U[22]. All the U-series ages were corrected for the initial ^{230}Th contamination assuming an initial $^{230}Th/^{232}Th$ activity ratio of 0.8±0.4, which is a value for a material at secular equilibrium with the bulk Earth upper crustal $^{232}Th/^{238}U$ atomic ratio of ~3.8[23].

The U-series dating were also done for the mammalian/human fossils in comparison (S-Fig. 1,2; S-Table 1-3).

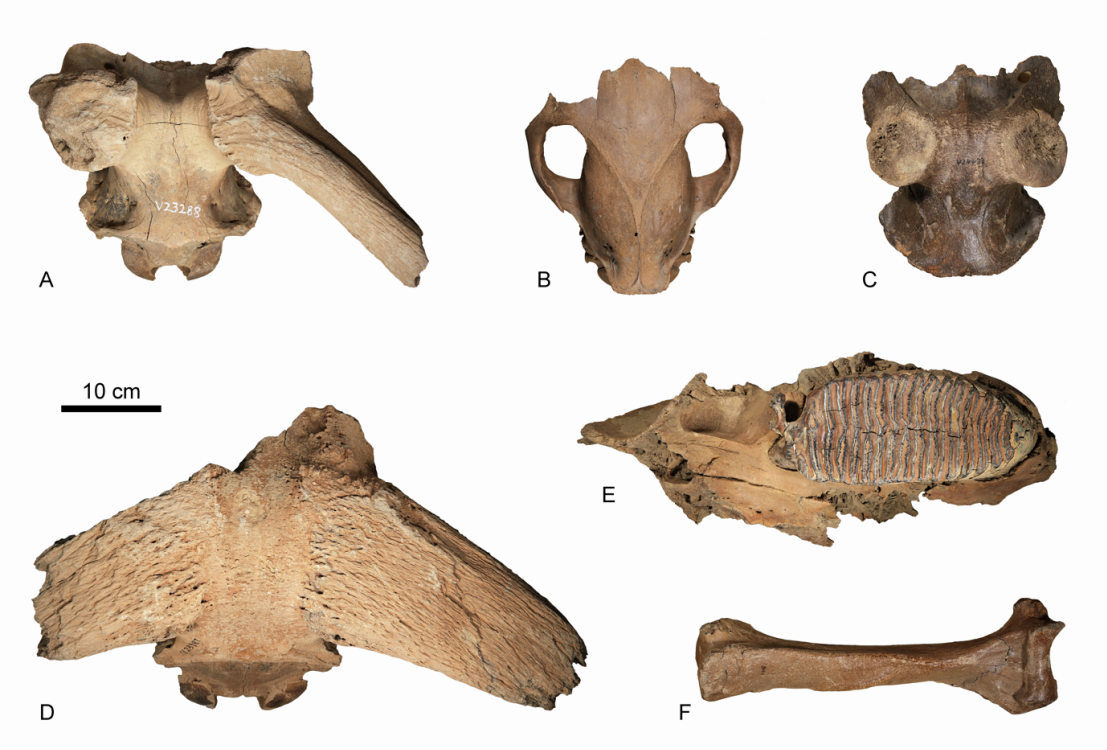

S-Figure 1. Middle-Late Pleistocene mammalian and human fossils from the Harbin area used for rare earth element concentration analyses and Sr isotopic analyses. A. V 23288, *Sinomegaceros ordosianus*. B. V 27805, *Equus przewalskii*. C. V 24433, *Cervus canadensis*. D. V 23987, *Bubalus wansjocki*. E. V 27804, *Mammuthus primigenius*. F. BH1, *Ursus arctos*.

S-Figure 2. Late Pleistocene-Early Holocene human fossils from the Harbin area used for rare earth element concentration analyses and Sr isotopic analyses. A. PA 1686. B. PA 1682.

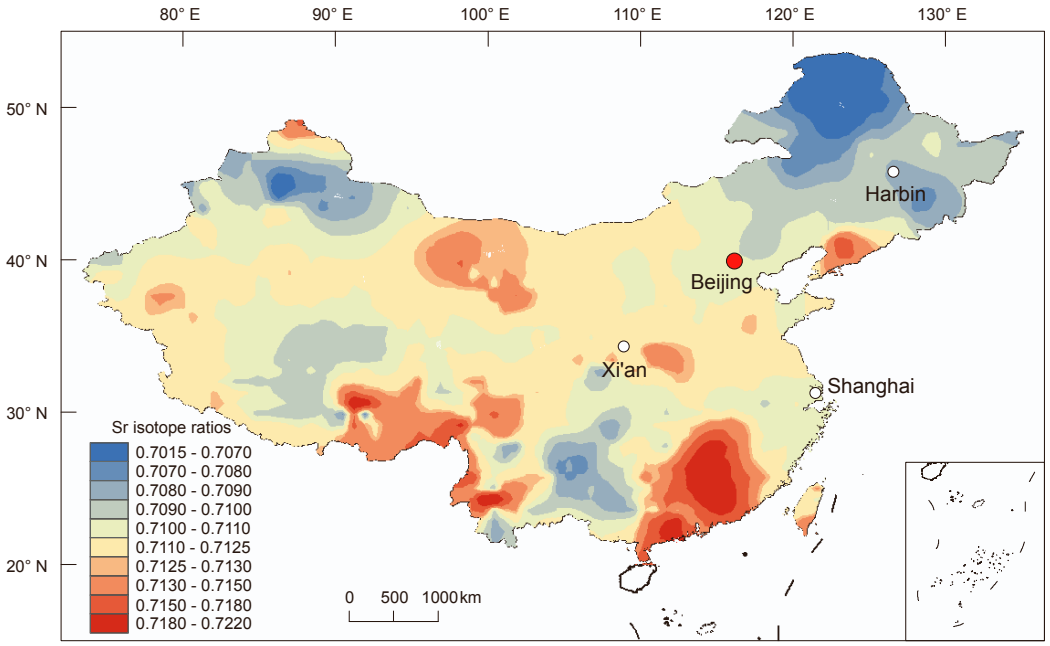

S-Figure 3. Large scale bioavailable Sr isotope map of China (data from the ref. [24], with permission).

S-Table 1. Concentrations (μg/g) of rare earth elements (REE) of the Harbin cranium in comparison with that of the Middle Pleistocene-Early Holocene human/mammalian fossils from the Harbin area

	Mammalian fossils					Human fossils			PAAS
Samples	V27805	V23987	V24433	V27804	V23288	PA1682	PA1686	Harbin cranium	
U-series Age (ka)	12±1	23.4±0.3	201±1	34.6±0.3	297±2†	9±4	17±3	148±2	
La	29.930	27.683	23.166	5.702	7.783	0.903	1.431	44.671	38.200
Ce	59.063	45.503	42.417	11.011	15.525	1.564	2.680	82.219	79.600
Pr	5.627	4.779	4.124	1.155	1.459	0.159	0.272	8.612	8.830
Nd	24.960	21.560	19.202	4.975	6.591	0.772	1.197	38.181	33.900
Sm	5.357	4.650	4.291	1.078	1.536	0.178	0.280	8.848	5.550
Eu	1.430	1.155	0.917	0.253	0.369	0.048	0.068	1.798	1.080
Gd	6.110	5.786	6.022	1.322	2.359	0.229	0.345	11.911	4.660
Tb	0.677	0.677	0.865	0.185	0.348	0.034	0.052	1.835	0.774
Dy	6.540	7.161	5.695	1.116	2.379	0.218	0.327	12.302	4.680
Ho	1.225	1.413	1.417	0.242	0.584	0.057	0.073	2.973	0.991
Er	4.398	5.371	4.491	0.703	1.819	0.176	0.222	9.383	2.850
Tm	0.527	0.671	0.636	0.100	0.259	0.025	0.031	1.361	0.405
Yb	3.056	4.069	4.047	0.617	1.586	0.171	0.192	8.951	2.820
Lu	0.545	0.755	0.709	0.099	0.270	0.032	0.032	1.536	0.433
LREE/HREE*	5.476	4.066	3.941	5.514	3.463	3.845	4.651	3.668	9.491
ΣREE**	149.445	131.233	117.997	28.557	42.867	4.566	7.203	234.580	167.160

*LREE is total content of light rare earth elements (LREE = La + Ce + Pr + Nd + Sm + Eu); HREE is total content of heavy rare earth elements (HREE = Gd + Tb + Dy + Ho + Er + Tm + Yb + Lu). **ΣREE is total content of rare earth elements (ΣREE = LREE +HREE).

† U-leaching cannot be excluded

S-Table 2. Sr isotope composition of the Harbin cranium and the adherent sediments in comparison with that of the Middle Pleistocene-Early Holocene human/mammalian fossils from the Harbin

Sample	V27805	V23987	V24433	V23288	V27804	F12	BH1	PA1686	PA1682	Harbin Cranium	Adherent sediments
U-series Ages (ka)	12.0±1	23.4±0.3	201±1	297±2†	34.6±0.3	340±3†	132.6±0.4	17±3	9±4	148±2	
$^{87}Sr/^{86}Sr$	0.709267	0.709574	0.709186	0.709137	0.709066	0.709411	0.709371	0.709165	0.709351	0.709423	0.711898
StdErr(2σ)	0.000010	0.000010	0.000010	0.000009	0.00010	0.000003	0.000004	0.000009	0.000009	0.000009	0.000003

† U-leaching cannot be excluded

S-Table 3. MC-ICPMS U-series dating results obtained on the Harbin cranium and Middle Pleistocene- Holocene mammalian and human fossils discovered in the Songhua River near the Harbin City, with uncertainties given at ±2σ level

Samples	U (μg/g)	Th (μg/g)	$^{234}U/^{238}U$	$^{230}Th/^{234}U$	$^{232}Th/^{238}U$ *	$^{230}Th/^{232}Th$	Age (ka b2k) **	Corr. $^{230}Th/^{234}U$***	Corr. Age (ka b2k) ***	$(^{234}U/^{238}U)_i$****
Harbin cranium										
HH19-1	10.28±0.02	2.929±0.008	1.548±0.005	0.474±0.003	0.0933±0.0006	7.86±0.03	66.9±0.5	0.446±0.015	62±3	1.65±0.01
HH19-2	7.64±0.02	3.042±0.008	1.566±0.007	0.593±0.004	0.1303±0.0008	7.13±0.03	91.5±0.9	0.562±0.017	85±4	1.72±0.01
HH19-3	8.99±0.02	5.96±0.01	1.503±0.004	1.039±0.004	0.2170±0.0009	7.20±0.02	305±6	1.031±0.006	296±8	2.16±0.03
HH19-4	5.191±0.003	1.174±0.002	1.481±0.002	0.798±0.002	0.0740±0.0002	15.97±0.04	151.7±0.7	0.787±0.006	148±2	1.73±0.01
HH19-5	4.850±0.004	2.462±0.003	1.519±0.003	0.973±0.003	0.1661±0.0005	8.90±0.02	241±2	0.962±0.006	233±5	2.00±0.01
HH19-6	9.958±0.005	0.629±0.001	1.503±0.002	0.653±0.001	0.0207±0.0001	47.5±0.1	106.6±0.4	0.649±0.003	106±1	1.678±0.003
HH19-7	3.971±0.003	0.669±0.001	1.508±0.003	0.950±0.002	0.0551±0.0002	25.98±0.06	225±2	0.946±0.003	223±2	1.95±0.01
HH20-1	5.212±0.002	0.922±0.005	1.543±0.001	0.984±0.001	0.0579±0.0003	26.2±0.1	248±1	0.981±0.002	245±2	2.08±0.01
HH20-2	9.729±0.004	1.097±0.006	1.508±0.001	0.738±0.001	0.0369±0.0002	30.1±0.2	130.7±0.3	0.731±0.003	129±1	1.730±0.003
HH20-3	2.562±0.001	0.666±0.003	1.576±0.001	0.891±0.001	0.0850±0.0005	16.50±0.09	188.6±0.6	0.882±0.004	185±2	1.97±0.01
Human and mammalian fossils collected from the Harbin area										
PA 1682	0.3094±0.0001	0.105±0.001	1.456±0.001	0.1339±0.0003	0.1111±0.0007	1.75±0.01	15.49±0.04	0.076±0.031	9±4	1.467±0.005
PA 1686	0.0951±0.0002	0.0325±0.0001	1.539±0.007	0.199±0.002	0.112±0.001	2.74±0.02	23.8±0.3	0.148±0.027	17±3	1.57±0.01
V 27805	5.049±0.001	0.362±0.004	1.516±0.001	0.117±0.002	0.023±0.001	7.5±0.2	13.4±0.2	0.105±0.006	12±1	1.534±0.001
V 23987	3.922±0.001	0.145±0.001	1.566±0.001	0.2010±0.0003	0.0121±0.0001	25.9±0.1	24.07±0.04	0.196±0.003	23.4±0.3	1.604±0.001
V 27804	2.286±0.001	0.0619±0.0003	1.468±0.001	0.2801±0.0005	0.0089±0.0001	46.4±0.3	35.1±0.1	0.276±0.002	34.6±0.3	1.517±0.002
BH1	9.237±0.003	0.126±0.001	1.429±0.001	0.740±0.001	0.00446±0.00004	237±2	132.8±0.4	0.739±0.001	132.6±0.4	1.624±0.002
V 24433	1.3481±0.0003	0.131±0.001	1.419±0.001	0.904±0.001	0.0317±0.0002	40.5±0.2	202.6±0.8	0.901±0.002	201±1	1.739±0.003
V 23288	0.3345±0.0001	0.0506±0.0003	1.460±0.001	1.028±0.002	0.0495±0.0003	30.3±0.2	299±2	1.026±0.002	297±2†	2.06±0.01
F12	39.413±0.007	0.143±0.001	1.205±0.001	1.011±0.001	0.00119±0.00001	1027±6	340±3	1.010±0.001	340±3†	1.536±0.004

* $^{232}Th/^{238}U$ activity ratios <0.1 indicates that the contamination of detrital ^{230}Th is insignificant for U-series age correction.

** U-series ages were calculated with half-lives of 75,584 yr for ^{230}Th (ref. [20]) and 245,620 yr for ^{234}U (ref. [20]), 1.4×10^{10} yr for ^{232}Th (ref. [21]), and 4.47×10^{9} yr for ^{238}U (ref. [22]). The ages are given at the "b2k" scale, before 2000 AD.

*** U-series ages were corrected with assumption of the initial $^{230}Th/^{232}Th$ atomic ratio of $4.4\pm2.2\times10^{-6}$, a value for a material at secular equilibrium, with the bulk earth $^{232}Th/^{238}U$ value of 3.8 and with an assumed error of 50%.

**** The back-calculated initial $^{234}U/^{238}U$ activity ratio.

† U-leaching cannot be excluded

References:

1. Bureau of Geology and Mineral Resources of Heilongjiang Province (BGMRHP), *Regional Geology of Heilongjiang Province*. People's Republic of China, Ministry of Geology and Mineral Resources, Geological Memoirs (Geological Publishing House, Beijing, 1993), vol. 33, pp. 734.
2. Wang, Y., Dong, J. and Yang, J. Quaternary Stratigraphy of the Huangshan Section in

Harbin. *Earth Science* **45**(7), 2662-2672 (2020).
3. Wei, Z., Xie, Y., Kang, C., Chi, Y., Wu, P., Wang, J., Zhang, M., Zhang, Y. and Liu, L. The Inversion of the Songhua River System in the Early Pleistocene: Implications from Sr-Nd isotopic composition in the Harbin Huangshan cores. *Acta Sedimentologica Sinica* **38**(6), 1192-1203 (2020). doi:10.14027/j.issn.1000-0550.2019.112
4. Zhan, T., Zeng, F., Xie, Y., Yang, Y., Ge, J., Ma, Y., Chi, Y., Kang, C., Jiang, X., Yu, Z., Zhang, J., Li, E. and Zhou, X. Magnetostratigraphic dating of a drill core from the Northeast Plain of China: Implications for the evolution of Songnen paleo-lake. *Chinese Science Bulletin* **64**(11), 1179-1190 (2019).
5. Institute of Vertebrate Paleontology CAS, *Pleistocene mammalian fossils from the northeastern provinces*. (Science Press, Beijing, 1959), pp. 82.
6. Zhengyi, W. The Quaternary mammalian fossils discovered in the Heilongjiang Province. , 1973, (01): 38-40. *Chinese Science Bulletin* **18**(1), 38-40 (1973).
7. Baoquan, C. and Jicai, Y. Late Pleistocene fossil mammals from Qinggang, Heilongjiang Province. *Bulletin of the Chinese Academy of Geological Sciences* **25**(131-138), (1992).
8. Huili, Y. and Wei, D. Pleistocene Mammalian fauna from the Jiaojie Cave at Acheng, Heilongjiang Province. *Quternary Science* **31**(4), 675-688 (2011).
9. Yang, Y., Li, Q., Fostowicz-Frelik, Ł. and Ni, X. Last record of *Trogontherium cuvieri* (Mammalia, Rodentia) from the late Pleistocene of China. *Quat. Int.* **513**, 30-36 (2019). doi:10.1016/j.quaint.2019.01.025
10. Ni, X., Li, Q., Stidham, T.A., Yang, Y., Ji, Q., Jin, C. and Samiullah, K. Earliest-known intentionally deformed human cranium from Asia. *Archaeological and Anthropological Sciences* **12**(4), 93 (2020). doi:10.1007/s12520-020-01045-x
11. Lu, D., Yang, Y., Li, Q. and Ni, X. A late Pleistocene fossil from Northeastern China is the first record of the dire wolf (Carnivora: *Canis dirus*) in Eurasia. *Quat. Int.*, (2020). doi:10.1016/j.quaint.2020.09.054
12. Li, J., Pei, R., Teng, F., Qiu, H., Tagle, R., Yan, Q., Wang, Q., Chu, X. and Xu, X. Micro-XRF study of the troodontid dinosaur *Jianianhualong tengi* reveals new biological and taphonomical signals. *Atomic Spectroscopy* **42**(1), 1-11 (2021).
13. Trueman, C.N., Behrensmeyer, A.K., Potts, R. and Tuross, N. High-resolution records of location and stratigraphic provenance from the rare earth element composition of fossil bones. *Geochimica et Cosmochimica Acta* **70**(17), 4343-4355 (2006). doi:10.1016/j.gca.2006.06.1556
14. Lei, H.-L., Yang, T., Jiang, S.-Y. and Pu, W. A simple two-stage column chromatographic separation scheme for strontium, lead, neodymium and hafnium isotope analyses in geological samples by thermal ionization mass spectrometry or multi-collector inductively coupled plasma mass spectrometry. *Journal of Separation Science* **42**(20), 3261-3275 (2019). doi:10.1002/jssc.201900579
15. Pin, C., Gannoun, A. and Dupont, A. Rapid, simultaneous separation of Sr, Pb, and Nd by extraction chromatography prior to isotope ratios determination by TIMS and MC-ICP-MS. *Journal of Analytical Atomic Spectrometry* **29**(10), 1858-1870 (2014).

doi:10.1039/C4JA00169A
16. Fourny, A., Weis, D. and Scoates, J.S. Comprehensive Pb-Sr-Nd-Hf isotopic, trace element, and mineralogical characterization of mafic to ultramafic rock reference materials. *Geochemistry, Geophysics, Geosystems* **17**(3), 739-773 (2016). doi:10.1002/2015GC006181
17. Douville, E., Sallé, E., Frank, N., Eisele, M., Pons-Branchu, E. and Ayrault, S. Rapid and accurate U–Th dating of ancient carbonates using inductively coupled plasma-quadrupole mass spectrometry. *Chemical Geology* **272**(1), 1-11 (2010). doi:10.1016/j.chemgeo.2010.01.007
18. Shao, Q.-F., Li, C.-H., Huang, M.-J., Liao, Z.-B., Arps, J., Huang, C.-Y., Chou, Y.-C. and Kong, X.-G. Interactive programs of MC-ICPMS data processing for ^{230}Th/U geochronology. *Quaternary Geochronology* **51**, 43-52 (2019). doi:10.1016/j.quageo.2019.01.004
19. Hiess, J., Condon, D.J., McLean, N. and Noble, S.R. ^{238}U/^{235}U Systematics in Terrestrial Uranium-Bearing Minerals. *Science* **335**(6076), 1610-1614 (2012).
20. Cheng, H., Lawrence Edwards, R., Shen, C.-C., Polyak, V.J., Asmerom, Y., Woodhead, J., Hellstrom, J., Wang, Y., Kong, X., Spötl, C., Wang, X. and Calvin Alexander, E. Improvements in ^{230}Th dating, ^{230}Th and ^{234}U half-life values, and U–Th isotopic measurements by multi-collector inductively coupled plasma mass spectrometry. *Earth and Planetary Science Letters* **371-372**, 82-91 (2013). doi:10.1016/j.epsl.2013.04.006
21. Holden, N.E. Total half-lives for selected nuclides. *Pure and Applied Chemistry* **65**(5), 941-958 (1990). doi:10.1351/pac199062050941
22. Goldstein, S.J., Murrell, M.T. and Janecky, D.R. Th and U isotopic systematics of basalts from the Juan de Fuca and Gorda Ridges by mass spectrometry. *Earth and Planetary Science Letters* **96**(1), 134-146 (1989). doi:10.1016/0012-821X(89)90128-3
23. Hans Wedepohl, K. The composition of the continental crust. *Geochimica et Cosmochimica Acta* **59**(7), 1217-1232 (1995). doi:10.1016/0016-7037(95)00038-2
24. Wang, X. and Tang, Z. The first large-scale bioavailable Sr isotope map of China and its implication for provenance studies. *Earth-Science Reviews* **210**, 103353 (2020). doi:10.1016/j.earscirev.2020.103353